Acta Cryst. (1998). A**54**, 606–616

X-ray Diffraction by a One-Dimensional Paracrystal of Limited Size

Xiang-Qi Mu

Institute of Molecular Biophysics, Florida State University, Tallahassee, FL 32306, USA. E-mail: mu@sb.fsu.edu

(*Received 25 August 1997; accepted 18 February 1998*)

Abstract

An explicit equation for X-ray diffraction by a finite one-dimensional paracrystal is derived. Based on this equation, the broadenings of reflections due to limited size and disorder are discussed. It depicts the paracrystalline diffraction over the whole reciprocal space, including the small-angle region where it degenerates into the Guinier equation for small-angle X-ray scattering. Positions of diffraction peaks by paracrystals are not periodic. Peaks shift to lower angles compared to those predicted by the average lattice constant. The shifts increase with increasing order of reflections and degree of disorder. If the heights and widths of the paracrystalline diffraction are treated as reduced quantities, they are functions of a single variable, $N^{1/2}g$. The width of the first diffraction depends mostly on size broadening for a natural paracrystal, where $N^{1/2}g = 0.1$–0.2. A method to measure the paracrystalline disorder and size using a single diffraction profile is proposed based on the equation of paracrystal diffraction. An initial value of size may be obtained using the Scherrer equation, that of the degree of disorder is then estimated by the α^* law. Final values of the parameters are determined through least-squares refinement against observed profiles. An equation of diffraction by a polydisperse one-dimensional paracrystal system is presented for 'box' distribution of sizes. The width of the diffraction decreases with increasing breadth of the size distribution.

1. Introduction

The classic theory of X-ray diffraction by one-dimensional paracrystals was founded by Zernike & Prins (1927) and was developed mainly by Hosemann and coworkers (Hosemann & Bagchi, 1962; Vainstein, 1966). Many studies of the second kind of disorder within polymers have been carried out in the light of this theory during the last decades (Baltá-Calleja & Vonk, 1989). The equation widely used for investigating diffraction by a one-dimensional paracrystal was derived assuming an infinitely large size (Vainstein, 1966; Baltá-Calleja & Vonk, 1989). Many natural paracrystals, however, have only limited length. For example, some observations on the paracrystal size match an empirical relation, called the α^* law (Baltá-Calleja & Hosemann, 1980). It says that $N^{1/2} = \alpha^*/g$, where N is the number of subunits in the system and g is the degree of disorder. α^* is usually small (between 0.1 and 0.2), with 0.14 as average. The number of subunits in a natural paracrystal with $g = 0.05$ is therefore only about 8, far from 'infinitely large'. Consequently, the size effect on the paracrystal diffraction has to be taken into consideration for a real substance. The method of Bonart *et al.* (1963) may separate its contribution to the diffraction width from that of disorder approximately. A formula is lacking for the diffraction profile by a finite paracrystal.

In an article on the basis of the statistical concept of a paracrystal model, Brämer (1975) obtained some results for diffraction by a finite one-dimensional paracrystal following the classic approach involving multiple convolutions. Expressed as the real part of some complex numbers, his formula did not develop any insight into the one-dimensional paracrystal diffraction.

Here, an explicit formula for X-ray diffraction by a one-dimensional paracrystal is derived through a more straightforward approach. The equation describes the paracrystal diffraction over the whole reciprocal space, including the small-angle region. It is applicable over a wide range of crystallite size and degree of disorder. A method to measure the degree of disorder and the paracrystal size using a single diffraction peak is proposed based on this formula. Furthermore, it reveals a series of new features of paracrystal diffraction.

2. Theory

The Fourier transform of a one-dimensional structure composed of N subunits is

$$F(X) = \sum_{k=1}^{N} \exp(2\pi i x_k X), \tag{1}$$

where x_k is the position of the kth subunit and X is the reciprocal-space coordinate. For simplicity, the subunit is assumed to be a point atom with a scattering factor of one. The intensity of X-ray diffraction by this system is then

$$I(X) = \sum_{k=1}^{N} \sum_{k'=1}^{N} \exp[2\pi i(x_k - x_{k'})X]. \tag{2}$$

ISSN 0108-7673

If an 'averaged lattice' exists for a one-dimensional paracrystal, the location of its kth atom may be written as

$$x_k = ka + \sum_{j=1}^{k} g_j a, \tag{3}$$

where a is the lattice constant of the 'average lattice' and g_j is an uncorrelated Gaussian random variable with zero mean.

Substitution of (3) into (2) gives

$$I(h) = \sum_{k=1}^{N}\sum_{k'=1}^{N} \exp[2\pi i(k-k')h] \times \exp\left[2\pi i\left(\sum_{j=1}^{k} g_j - \sum_{j'=1}^{k'} g_{j'}\right)h\right], \tag{4}$$

where

$$h = aX \tag{5}$$

is the continuous reciprocal-space coordinate in units of $1/a$. Each term within the double summation in (4) is connected only with the difference between k and k'. There are N terms with $k = k'$, $N-1$ terms with $k-k' = 1$, $N-1$ terms with $k-k' = -1$, $N-2$ terms with $k-k' = 2$ and the same with $k-k' = -2, \ldots$. After grouping the terms with the same differences between k's, the double summation in (4) may be replaced with a single one:

$$I(h) = N + \sum_{k=1}^{N-1}(N-k)\left[\exp(2\pi ikh)\exp\left(2\pi ih\sum_{j=1}^{k} g_j\right) + \exp(-2\pi ikh)\exp\left(-2\pi ih\sum_{j=1}^{k} g_j\right)\right]. \tag{6}$$

The intensity $I(h)$, as shown, depends on details of the distribution of atoms in the system. Observed intensities, however, are those averaged over the random variable g_j. It is known (Barakat, 1987) that the average of the g_j-related part in (6) may be expressed with the aid of $\langle g^2\rangle$, the variance of g_j:

$$\left\langle \exp\left(\pm 2\pi ih\sum_{j=1}^{k} g_j\right)\right\rangle = \exp(-2\pi^2 h^2 k\langle g^2\rangle). \tag{7}$$

The averaged X-ray diffraction intensity by a one-dimensional paracrystal is then

$$\langle I(h)\rangle = N + \sum_{k=1}^{N-1}(N-k)[\exp(2\pi ikh) + \exp(-2\pi ikh)] \times \exp(-2\pi^2 h^2 k\langle g^2\rangle). \tag{8}$$

Two new parameters are introduced for convenience:

$$\alpha = 2\pi h \tag{9}$$

$$\beta = \exp(-2\pi^2 h^2 g^2), \tag{10}$$

where $\langle g^2\rangle^{1/2}$ is simplified as g and is called the degree of disorder of the paracrystal. We may rewrite (8) as

$$\langle I(\alpha)\rangle = N + 2\sum_{k=1}^{N-1}(N-k)\beta^k \cos k\alpha. \tag{11}$$

Explicit forms of the two summations in this equation were derived with the aid of the following formulas (Gradshteyn & Ryzhik, 1980):

$$\sum_{k=1}^{N-1}\beta^k \cos k\alpha = [\beta\cos\alpha - \beta^2 - \beta^N\cos N\alpha + \beta^{N+1}\cos(N-1)\alpha] \times (1 - 2\beta\cos\alpha + \beta^2)^{-1} \tag{12}$$

$$\sum_{k=1}^{N-1}\beta^k \sin k\alpha = [\beta\sin\alpha - \beta^N\sin N\alpha + \beta^{N+1}\sin(N-1)\alpha] \times (1 - 2\beta\cos\alpha + \beta^2)^{-1}. \tag{13}$$

Multiplying both sides of (12) by N, we obtain the first summation in (11). Starting from derivatives of (12) and (13) with respect to α, we get the second summation after a tedious, but not difficult, derivation. The final explicit equation for the diffraction intensity by a one-dimensional paracrystal is

$$\langle I(\alpha)\rangle = [N(1-\beta^2)](1 - 2\beta\cos\alpha + \beta^2)^{-1} - [2\beta(\cos\alpha - 2\beta + \beta^2\cos\alpha)] \times (1 - 2\beta\cos\alpha + \beta^2)^{-2} + \{2\beta^{N+1}[\cos(N+1)\alpha - 2\beta\cos N\alpha + \beta^2\cos(N-1)\alpha]\}(1 - 2\beta\cos\alpha + \beta^2)^{-2}. \tag{14}$$

The intensity is obviously continuous in reciprocal space. By removal of the disorder from the system, an ideal one-dimensional crystal appears, where N point atoms are separated exactly by the constant a. Diffraction intensity by this ideal system should be a series of δ functions separated by $1/a$ in reciprocal space and with a height of N^2. The ratio of diffraction intensities by a paracrystal and an ideal crystal at a reciprocal-lattice point is

$$\langle i(\alpha)\rangle = (1/N)(1-\beta^2)(1 - 2\beta\cos\alpha + \beta^2)^{-1} - (1/N^2)[2\beta(\cos\alpha - 2\beta + \beta^2\cos\alpha)] \times (1 - 2\beta\cos\alpha + \beta^2)^{-2} + (1/N^2)\{2\beta^{N+1}[\cos(N+1)\alpha - 2\beta\cos N\alpha + \beta^2\cos(N-1)\alpha]\}(1 - 2\beta\cos\alpha + \beta^2)^{-2}. \tag{15}$$

This is, therefore, the reduced diffraction intensity by a one-dimensional paracrystal. Substitution of $\alpha = 2\pi n$, where n is an integer, into this equation gives

$$\langle i(2n\pi)\rangle = (1/N)[(1+\beta_n)/(1-\beta_n)] - (1/N^2)[2\beta_n/(1-\beta_n)^2] + (1/N^2)[2\beta_n^{N+1}/(1-\beta_n)^2], \quad (16)$$

where $\beta_n = \exp(-2\pi^2 n^2 g^2)$. The new equation represents the nth-order paracrystal diffraction.

3. Results

The diffraction intensities by finite one-dimensional paracrystals with $N^{1/2}g$ of 0.14 are calculated using (15) for degree of disorder 0.007, 0.05, 0.08 and 0.10, respectively, over a range of α from 0 to 20π. They are shown in Fig. 1. The intensities are almost discrete for small g. They decrease significantly with increasing α even when the degree of disorder is very small. Widths of diffractions increase quickly with increasing α and/or g. High background emerges for large α and/or large g. Fig. 2 shows curves of $\langle i(\alpha)\rangle$ against α (thick lines) for $g = 0.05$ with various N, *i.e.* $N^{1/2}g$ are 0.10, 0.14, 0.2 and 1.0 in (*a*), (*b*), (*c*) and (*d*), respectively. The width of curve $\langle i(\alpha)\rangle$, as shown, increases with decreasing size. All these results are more or less consistent with previous studies (Hosemann & Bagchi, 1962; Baltá-Calleja & Vonk, 1989).

New insights into the paracrystal diffraction are also developed based upon (15). They are described below.

3.1. *Approximations of equation (15)*

The most important application of the classic theory is the prediction of the width of diffraction by a one-dimensional paracrystal. The diffraction of a paracrystal with very large size is (Vainstein, 1966; Baltá-Calleja & Vonk, 1989)

$$\langle i(\alpha)\rangle = \frac{1}{N}\frac{(1-\beta^2)}{(1-2\beta\cos\alpha+\beta^2)}. \quad (17)$$

The integral width of nth-order diffraction is $\pi^2 n^2 g^2$ according to this equation.

Equation (17) corresponds to the first term of (15). On the right-hand side of (15), the first term is $1/N$ dependent, while the second and third are $1/N^2$ dependent. It is obvious that (15) degenerates into (17) when N is very large.

Diffraction curves calculated using (17) are shown with broken lines in Fig. 2. As mentioned above, the continuous lines represent those calculated using (15). Peaks calculated with (17) are always higher and narrower, compared to those using (15). The difference is large for natural paracrystals where $N^{1/2}g$ is equal to 0.14, as shown in Fig. 2(*b*); it is significant even when $N^{1/2}g$ is equal to 0.2, the upper limit of α^*, as shown in Fig. 2(*c*). Except for the small-angle part, the diffraction pattern may be approximated using (17) only when $N^{1/2}g$ is close to 1, as seen in Fig. 2(*d*).

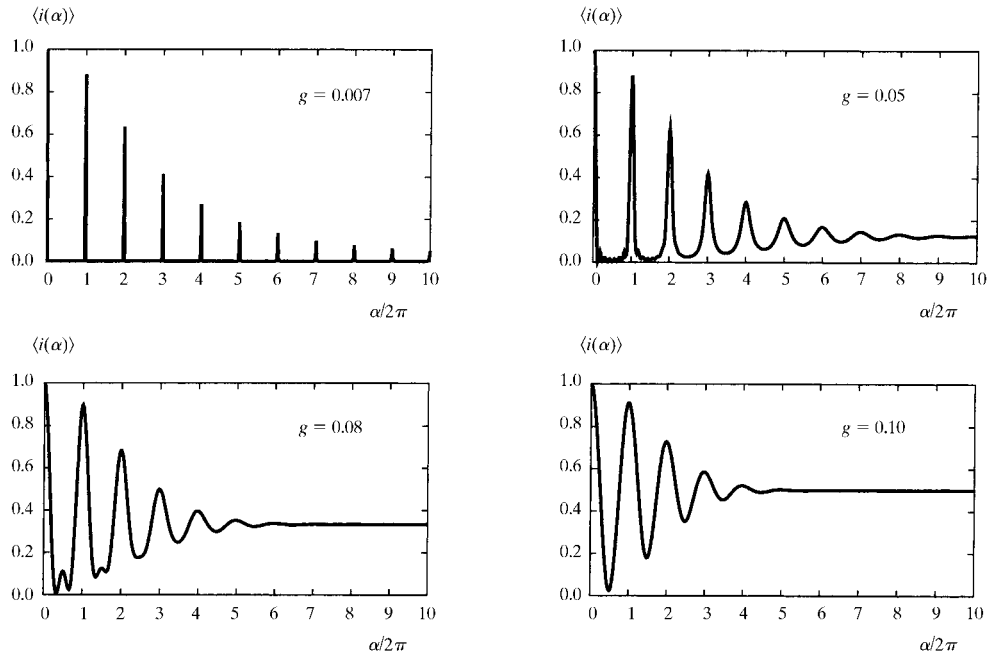

Fig. 1. Curves of $\langle i(\alpha)\rangle$ *vs* α for finite paracrystals ($N^{1/2}g = 0.14$) with degrees of disorder of 0.007, 0.05, 0.08 and 0.10, respectively. The sizes of the structures are $N = 400$, 8, 3 and 2 respectively. $\langle i(2\pi)\rangle$ is the most intense observable in a diffraction pattern. It is, however, always lower than $\langle i(0)\rangle$, which is equal to 1.0. Intensities decrease with increasing α. Widths of diffraction increase with increasing g and α. The background increases quickly with α for larger g.

The error of the approximated equation (17) may be estimated over the range of the first peak, the most important part of paracrystal diffraction data. The R factor may be defined as

$$R = \sum_{\alpha=\alpha_1}^{\alpha_2} |I_{(15)}(\alpha) - KI_{(17)}(\alpha)| \Big/ \sum_{\alpha=\alpha_1}^{\alpha_2} I_{(15)}(\alpha), \qquad (18)$$

where $I_{(15)}(\alpha)$ and $I_{(17)}(\alpha)$ are the first-order diffraction calculated using (15) and (17), respectively. The range of the summation, $\alpha_2 - \alpha_1$, should cover the whole peak. The constant K is adjusted so that the areas under the curves are the same for $I_{(15)}(\alpha)$ and $I_{(17)}(\alpha)$.

Curves of R against $N^{1/2}g$ are calculated for degree of disorder from 0.01 to 0.10. All the curves, regardless of the magnitude of g, are similar. As a representative, the curve for $g = 0.06$ is shown in Fig. 3. The R factor for the lower and upper limits of α^*, *i.e.* $N^{1/2}g = 0.1$ and 0.2, are 1.22 and 0.68, respectively. It is obvious that X-ray diffraction by a natural paracrystal cannot be approximated by (17).

Another approximation for paracrystal diffraction is

$$\langle i(\alpha)\rangle = \frac{1}{N}\frac{(1-\beta^2)}{1-2\beta\cos\alpha+\beta^2} - \frac{1}{N^2}\frac{2\beta(\cos\alpha - 2\beta + \beta^2\cos\alpha)}{(1-2\beta\cos\alpha+\beta^2)^2}. \qquad (19)$$

This is obtained by omission of only the third term of (15). Curves of $\langle i(\alpha)\rangle$ against α in the region of the first-order diffraction are shown in Figs. 4(*a*), (*b*), (*c*) and (*d*) and correspond with $N^{1/2}g = 0.14$, 0.25, 0.35 and 1.0, respectively. The thick lines in the figures represent the peaks calculated using (15) and the thin, broken and dotted lines are the contributions from the first term, summations of first and second terms and the third term, respectively. When $N^{1/2}g$ is 0.35, the contribution of the third term is very small, the sum of the other two terms provides a close approximation for the one-dimensional paracrystal diffraction, as shown in Fig. 4(*c*).

3.2. *Background*

As shown in Fig. 1, the background of paracrystal diffraction increases with increasing g and increasing α. We may estimate the background by substitution of $\alpha = (2n-1)\pi$, the midpoint between diffraction peaks, into (15). The third term can be ignored when n and/or N is large. We have, therefore,

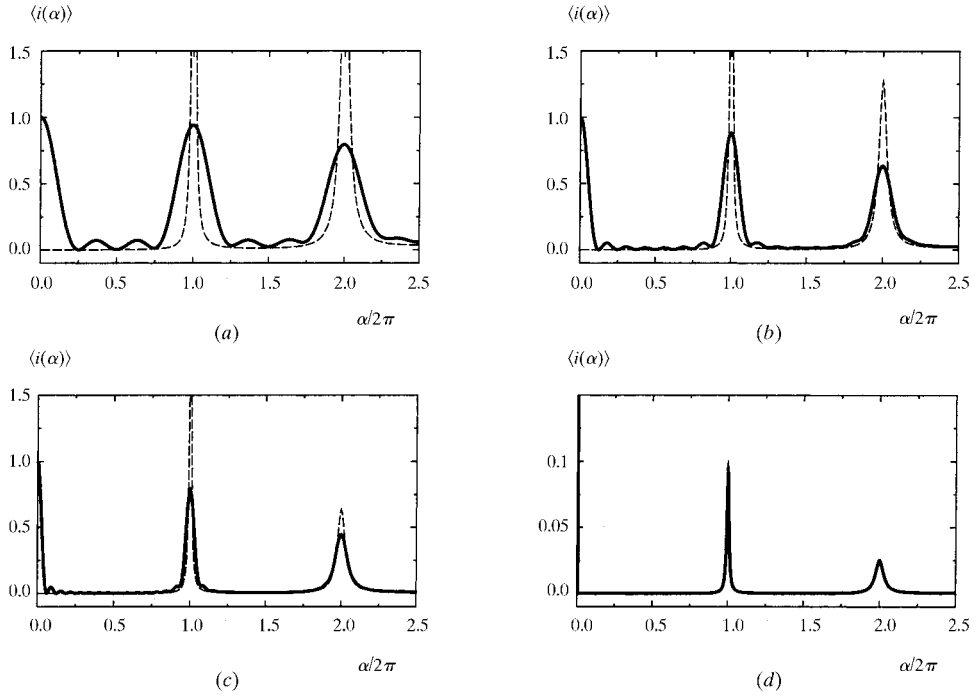

Fig. 2. Curves of $\langle i(\alpha)\rangle$ *vs* α (thick solid lines) for paracrystals with $g = 0.05$ and $N = 4, 8, 16$ and 400 as shown in (*a*), (*b*), (*c*) and (*d*), respectively. Note that the scale of $\langle i(\alpha)\rangle$ in (*d*) is ten times less than that in the others. Both peaks and widths of diffractions decrease with increasing N. Curves marked by broken lines are calculated using equation (17) or the first term of equation (15). They differ from thick solid lines, calculated using (15), in that (i) they are always higher and narrower, (ii) they have negligible value in the small-angle region, and (iii) there is no ripple between peaks. The difference between the two kinds of curves is large for a natural paracrystal, where $N^{1/2}g \leq 0.2$; it may be neglected only when $N^{1/2}g$ is close to 1.0, where the two curves are almost identical except in the small-angle region.

$$\langle i(2n\pi - \pi)\rangle = \frac{1}{N}\frac{1-\beta}{1+\beta} + \frac{1}{N^2}\frac{2\beta}{(1+\beta)^2}. \qquad (20)$$

Refer to Fig. 1; if curves are drawn by connecting the minima of $\langle i(\alpha)\rangle$, they will match this equation. As shown in both the figure and the equation, the background of one-dimensional paracrystal diffraction asymptotically approaches $1/N$ at high angle.

3.3. *Peak shift*

It is remarkable that the diffraction peaks by a paracrystal are not periodic. For example, the six peaks for the paracrystal with $g = 0.05$ and $N^{1/2}g = 0.14$ (see Fig. 1) are located at 0.9994, 1.9986, 2.9974, 3.9954, 4.9924 and 5.9890, respectively. None is located exactly at a multiple of 2π or a multiple of $1/a$, the latter is the average reciprocal-lattice constant. The position of the nth-order diffraction peak may be written as

$$h_n = n - \delta_n, \qquad (21)$$

where δ_n, called the peak shift, takes small positive values. These can be obtained in diffraction profiles calculated using (15). δ_n depends on the values of N, g and n. It increases with increasing g, increasing n and decreasing N. The curves of δ_n against n for $N^{1/2}g = 0.14$, $g = 0.02$, 0.04, 0.06, 0.08 and 0.10 are shown in Fig. 5 (solid lines).

The peak shift of paracrystal diffraction may be observed even in calculated diffraction profiles using the approximated equation (17) (Hosemann, 1962). Equation (17) may represent paracrystal diffraction only when N is very large. Consequently, the peak shift obtained from (17) should be its lower limit for specific g and n. The limit of δ_n, δ'_n, can also be calculated directly from (17). Taking the derivative of (17) with respect to α and setting it equal to zero, we have

$$g^2\alpha_n(\cos\alpha_n - 2\beta_n + \beta_n^2\cos\alpha_n) = (\beta_n^2 - 1)\sin\alpha_n, \qquad (22)$$

where $\alpha_n = 2\pi(n - \delta'_n)$, the peak position of nth-order diffraction. The trigonometric functions in the equation can be simplified because δ'_n is small: $\cos\alpha_n = 1$ and $\sin\alpha_n = -2\pi\delta'_n$. Substitution of these approximations into (22) gives immediately

$$\delta'_n = ng^2(1 - \beta_n)/(1 + \beta_n). \qquad (23)$$

Curves of δ'_n against n calculated using this equation are shown in Fig. 5 also (dashed lines). The two kinds of curves (solid lines and dashed lines) are closer for smaller g or higher n. They coincide with each other when g is less 0.04. In other words, δ_n is N independent for small g (< 0.04). When g is big, a smaller size of the paracrystal may cause a larger peak shift.

Similarly, the minima of paracrystal diffraction are not periodic either. The approximated shift can be obtained by (17) too:

$$h_{n-1/2} = (n - \tfrac{1}{2}) - \delta'_{n-1/2}, \qquad (24)$$

where $\delta'_{n-1/2}$ is another positive small number:

$$\delta'_{n-1/2} = (n - \tfrac{1}{2})g^2(1 + \beta_{n-1/2})/(1 - \beta_{n-1/2}). \qquad (25)$$

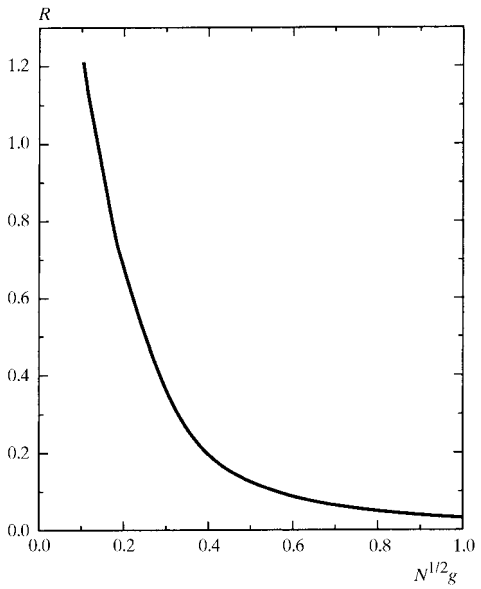

Fig. 3. Curve of R against $N^{1/2}g$ when $g = 0.06$. The R factor represents the error given by the approximate formula (17), estimated based on first-order diffraction. It is very large for a finite paracrystal. Paracrystal diffraction cannot be approximated by equation (17).

3.4. *Small-angle scattering*

As shown in Fig. 2 (thick lines), (15) predicts reasonable small-angle scattering for a paracrystal. They are always the most intense reflections in the pattern. The formula for small-angle scattering by a one-dimensional paracrystal can also be derived from (15). When α is close to zero, all the exponential and trigonometric functions in the equation approach 1 at higher or lower speed. Equation (15) can then be greatly simplified. In the small-angle region, we have $\cos\alpha = 1 - \alpha^2/2$; $\beta = 1 - g^2\alpha^2/2$; $\beta^N = 1 - Ng^2\alpha^2/2$ and

$$\cos N\alpha = 1 - \tfrac{1}{2}N^2\alpha^2 + \tfrac{1}{24}N^4\alpha^4. \qquad (26)$$

Substitution of these approximations into (15) results in

$$\langle i(\alpha)\rangle = 1 - \tfrac{1}{12}N^2\alpha^2. \qquad (27)$$

This equation is similar to the Guinier formula (Guinier, 1939) in that the small-angle X-ray scattering increases with decreasing squared angle.

Curves of $\langle i(\alpha)\rangle$ against α^2 in the small-angle range are shown in Figs. 6(a), (b), (c) and (d) for $g = 0.05$ and $N = 50$, 71, 87 and 100, respectively. Circles are calculated using (15), straight lines using the approximate equation (27).

3.5. *Diffraction as a function of $N^{1/2}g$*

The size effect on X-ray diffraction intensity by a paracrystal may be investigated theoretically over a wider range than that restricted by the α^* law. For example, the intensities of the first peak ($\alpha = 2\pi$) may be calculated for various values of g and N without limitation of $N^{1/2}g$. It is interesting that when $\langle i(2\pi)\rangle$ are drawn as curves against $N^{1/2}g$, all data points are matched with a single curve, as shown in Fig. 7(*a*). In other words, $\langle i(2\pi)\rangle$ is a function of a single variable, *i.e.* $N^{1/2}g$. The actual size of a paracrystal with N subunits is $Na \pm N^{1/2}ga$, where g is the degree of disorder, a is a constant of the 'average lattice'. $N^{1/2}ga$ may be regarded as the size fluctuation of the paracrystal. $N^{1/2}g$, the ratio of the fluctuation to the lattice constant, is the reduced size fluctuation of the system. The curve in Fig. 7(*a*) reflects a relationship between two reduced parameters. The axis of ordinates represents the reduced intensity, the ratio of the intensity from a paracrystal to that from an ideal crystal. The abscissa represents $N^{1/2}g$, the reduced size fluctuation.

As shown in Fig. 7(*a*), intensities $\langle i(2\pi)\rangle$ decrease with increasing $N^{1/2}g$. The rate of change, however, varies along the curve. The maximum rate of change occurs at a special point in the curve, the point of inflection. The

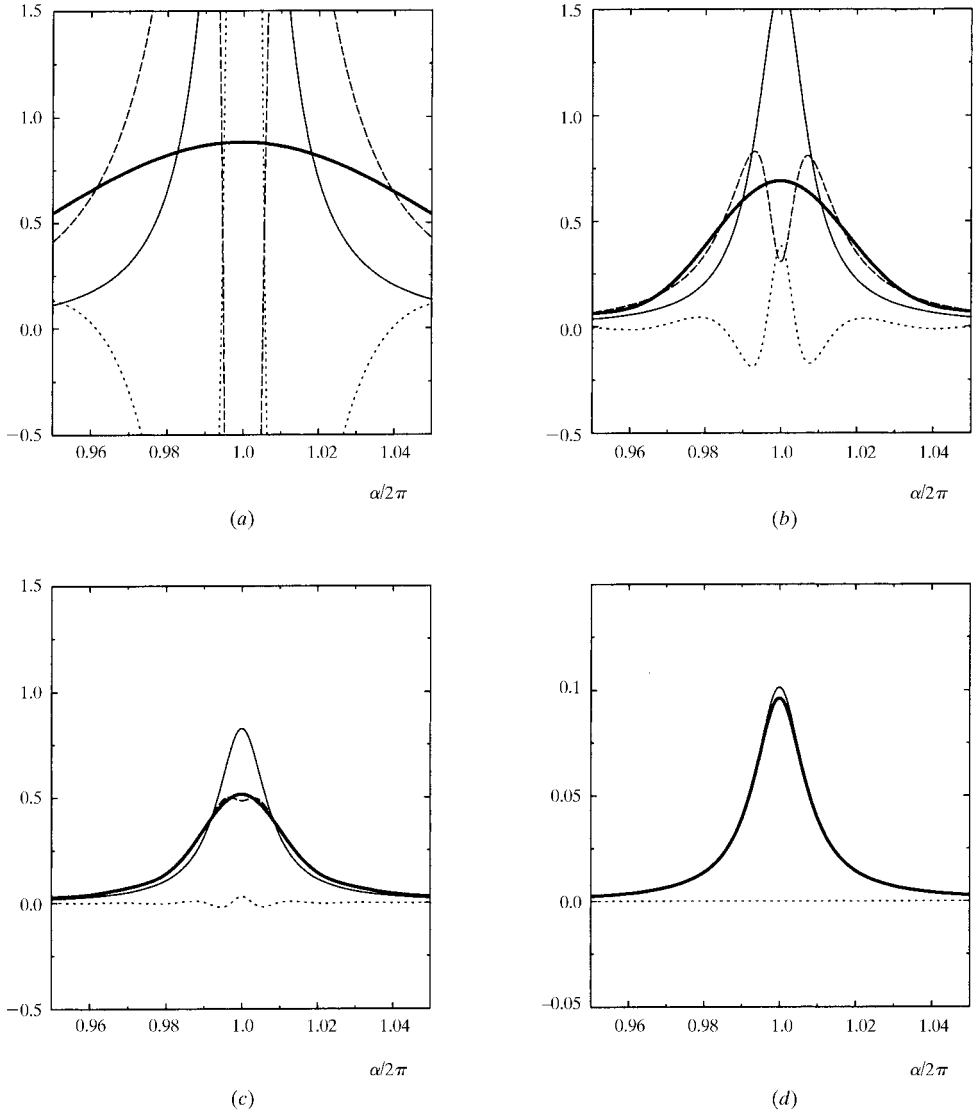

Fig. 4. Diffraction profile (thick lines) of first order ($\alpha = 2\pi$) compared to contributions from the first term (thin lines), the third term (dotted lines) and the first plus second terms (dashed lines) of equation (15). With a fixed degree of disorder g of 0.05, $N^{1/2}g$ is 0.14, 0.25 0.35 and 1.0 for (*a*), (*b*), (*c*) and (*d*), respectively. None of the three terms in equation (15) may be ignored to define the diffraction profile for a natural paracrystal when $N^{1/2}g$ is 0.1 to 0.2. The third term may be ignored when $N^{1/2}g$ is about 0.35, as shown in (*c*). Both second and third terms are ignored only when $N^{1/2}g$ is close to 1, as shown in (*d*).

derivative of $\langle i(2\pi)\rangle$ with respect to $N^{1/2}g$ reaches its minimum at this point, where $\langle i(2\pi)\rangle = 0.68$ and $N^{1/2}g = 0.244$, as shown in Fig. 7 (*b*).

3.6. *Width of diffraction as a function of* $N^{1/2}g$

Half-width, defined as the full width at half the maximum intensity and denoted by W, is used here as usual for convenience.

Diffraction by paracrystals with various parameters (N and g) were calculated using (15), and values of W were measured for peaks at $\alpha = 2\pi$, 4π and 6π on these curves. When W are plotted as a curve of W/π^2g^2 against $N^{1/2}g$, the data points for each peak follow a single curve. The curves for peaks 1, 2 and 3 are shown in Fig. 8. π^2g^2 reflects the broadening effect of the second kind of disorder. W/π^2g^2 is obviously a reduced width and it is also a function of single variable, $N^{1/2}g$. In practice, the curve for peak 1 is the most important, it fits the following empirical formula:

$$W/\pi^2g^2 = 0.256\,92 + 0.363\,15\,N^{1/2}g + 0.089\,462/Ng^2. \tag{28}$$

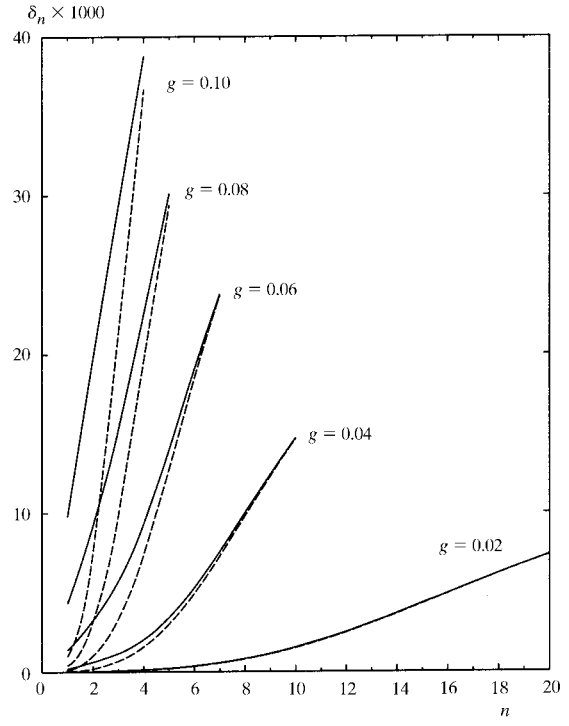

Fig. 5. Peak shift of nth-order paracrystal diffraction. The solid lines represent readings on a diffraction pattern calculated using equation (15) for a paracrystal with $N^{1/2}g = 0.14$. The dashed lines are from equation (23) for a paracrystal with $N^{1/2}g = 1$. The peak shift quickly increases with increasing g and increasing n.

For a natural paracrystal, where $N^{1/2}g$ is less than or equal to 0.2, the first and second terms in (28) may be neglected compared to the third. Equation (28) can then be approximated by

$$W/\pi^2g^2 \cong 0.089\,462/Ng^2 \tag{29}$$

or

$$W \cong 0.88/N. \tag{30}$$

This is the famous Scherrer equation (Scherrer, 1918) for measurement of crystallite size. The second kind of disorder makes only a very small contribution to the broadening of the first-order diffraction of a natural paracrystal. Practically, the paracrystal size may be estimated by the width of the first-order diffraction using the Scherrer equation.

3.7. *Distribution of paracrystal sizes*

Equation (15) is valid for monodisperse system, *i.e.* all paracrystals in the system have the same size. For a polydisperse system, only the diffraction, averaged over the radiated part of the sample, is observable. It may be described as

$$\overline{\langle i(\alpha)\rangle} = \sum_{\mathcal{N}=\mathcal{N}_{\min}}^{\mathcal{N}_{\max}} \langle i(\alpha)\rangle P(\mathcal{N}), \tag{31}$$

where $\mathcal{N}$ is a random integer variable, $P(\mathcal{N})$ is its probability distribution function, $\mathcal{N}_{\max}$ and $\mathcal{N}_{\min}$ are the upper and the lower limits of the sum, respectively. The first moment of $\mathcal{N}$,

$$\langle \mathcal{N}\rangle = \sum_{\mathcal{N}=\mathcal{N}_{\min}}^{\mathcal{N}_{\max}} \mathcal{N}P(\mathcal{N}), \tag{32}$$

is called the mean or the average size. Substitution of (15) and the specific form of $P(\mathcal{N})$ into (31) will result in a specific formula for the distribution function.

For example, a normalized 'box' distribution may be defined by

$$P(\mathcal{N}) = \begin{cases} 1/(2\Delta+1), & \langle\mathcal{N}\rangle - \Delta \le \mathcal{N} \le \langle\mathcal{N}\rangle + \Delta \\ 0, & \text{otherwise,} \end{cases} \tag{33}$$

where $\langle\mathcal{N}\rangle$ is the average size, 2Δ is the width of the distribution. When (15) and (32) are substituted into (31), one obtains

$$\begin{aligned} \overline{\langle i(\alpha)\rangle} = {} & \frac{1}{\langle\mathcal{N}\rangle}\frac{(1-\beta^2)}{1-2\beta\cos\alpha+\beta^2} \\ & - \frac{1}{\langle\mathcal{N}\rangle^2}\frac{2\beta(\cos\alpha - 2\beta + \beta^2\cos\alpha)}{(1-2\beta\cos\alpha+\beta^2)^2} \\ & + \frac{1}{\langle\mathcal{N}\rangle^2}\frac{2\beta^{\langle\mathcal{N}\rangle+1}}{(1-2\beta\cos\alpha+\beta^2)^3}\frac{T_3}{2\Delta+1}, \end{aligned} \tag{34}$$

where

$$T_3 = \beta^{\Delta+2}[\cos(\mathcal{N}_{\max}+1)\alpha - 2\beta\cos\mathcal{N}_{\max}\alpha + \beta^2\cos(\mathcal{N}_{\max}-1)\alpha] - \beta^{\Delta+1}[\cos(\mathcal{N}_{\max}+2)\alpha - 2\beta\cos(\mathcal{N}_{\max}+1)\alpha + \beta^2\cos\mathcal{N}_{\max}\alpha] - \beta^{-\Delta+1}[\cos\mathcal{N}_{\min}\alpha - 2\beta\cos(\mathcal{N}_{\min}-1)\alpha + \beta^2\cos(\mathcal{N}_{\min}-2)\alpha] + \beta^{-\Delta}[\cos(\mathcal{N}_{\min}+1)\alpha - 2\beta\cos\mathcal{N}_{\min}\alpha + \beta^2\cos(\mathcal{N}_{\min}-1)\alpha], \quad (35)$$

where $N_{\max} = \underline{\langle\mathcal{N}\rangle} + \Delta$, $N_{\min} = \langle\mathcal{N}\rangle - \Delta$.

Curves of $\langle i(\alpha)\rangle$ against α for $\langle\mathcal{N}\rangle = 16$, $g = 0.05$ and $\Delta = 0$, 4, 8, 12 and 16 are shown in Fig. 9. For a polydisperse system, the diffraction profile depends not only on the average size and the degree of disorder but also upon the size distribution. As shown in Fig. 9, the breadth of the diffraction profile decreases with increasing width of the size distribution. The ripples in the tail of the profile are smoothed out when the size distribution is not too narrow.

4. Applications

Two methods have been applied to measure the paracrystal size and the degree of disorder. The Fourier transform method (Warren & Averbach, 1950; Warren, 1959) is the most sound technologically. It requires, however, high-quality experimental data and special skill for data processing (Somashekar *et al.*, 1989; Hall & Somashekar, 1991). The integral breadth method (Baltá-Calleja & Vonk, 1989) is simple and convenient but assumptions regarding the relationship between the structural parameters (N and g) and the breadth of the peaks have to be made. A common difficulty in practice for both techniques is that two or more reflection orders are required. In many cases, however, only a single order is observed in diffraction by polymer material.

The explicit formula for X-ray diffraction by a paracrystal, equation (15) of this paper, makes it possible to refine the crystallite size and degree of disorder against the observed diffraction profile. Furthermore, single-order reflection may be enough for the refinement. Here

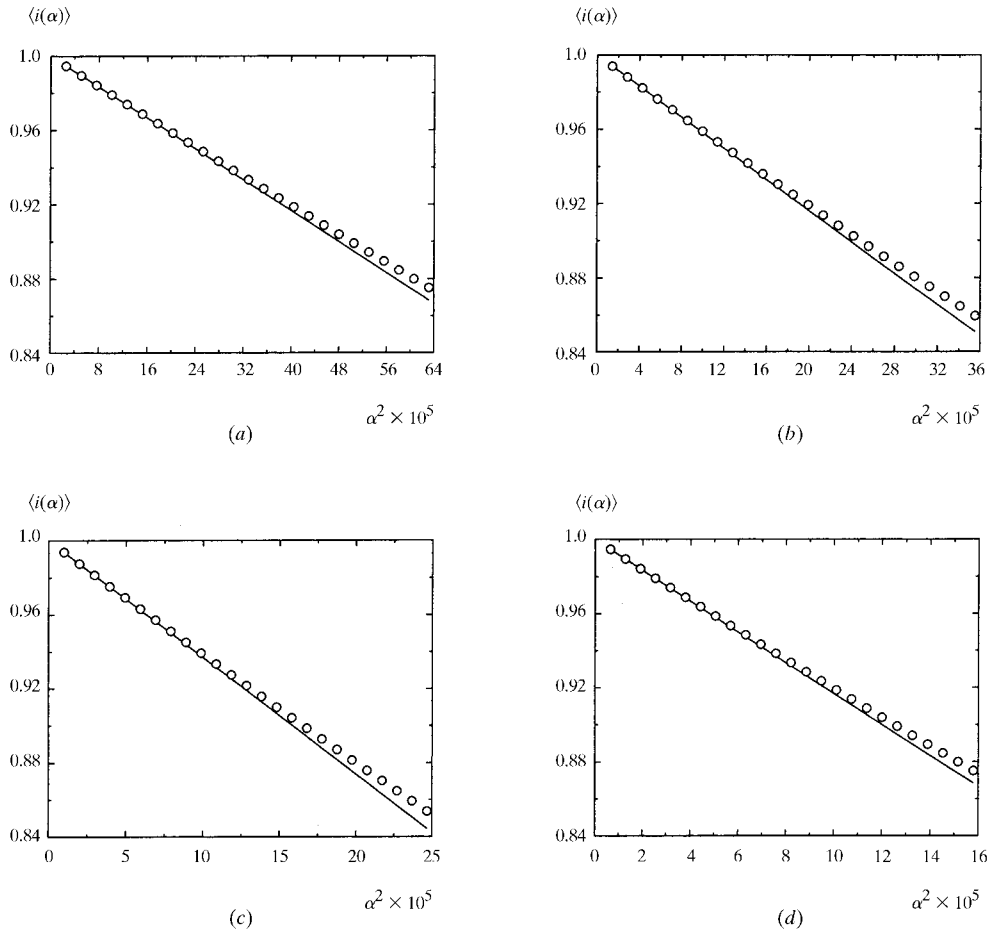

Fig. 6. Guinier plots, *i.e.* curves of $\langle i(\alpha)\rangle$ *vs* α^2 in the small-angle region of paracrystals with $g = 0.05$ and $N = 50$, 71, 87 and 100 for (*a*), (*b*), (*c*) and (*d*), respectively. Markers are calculated using equation (15), straight lines using equation (27).

we suggest a two-step procedure to carry out the measurement. First, an initial value of N is estimated from the width of the first-order reflection using (30), the Scherrer equation; the initial degree of disorder is then derived from the α^* law. Second, calculated diffraction data are obtained from the initial values of N and g using (15); the two parameters are then adjusted against observed diffraction until the best fit between the calculated diffraction and the observed is reached. This may be implemented using a standard least-squares technique.

The experimental profile of reflection 110 by polyethylene fiber is used to test the procedure. This curve is taken from Fig. 2 of Hall & Somashekar (1991). The ripple in the tail part of the curve indicates that the sample is likely to be a monodisperse system. In the first step, the initial values of the parameters are estimated as $N = 17$, $g = 0.034$. The simplex algorithm (Press *et al.*, 1986) is used to implement the refinement procedure. The final values of the parameters are $N = 17$ and $g = 0.0415$. The result is consistent with that of Hall & Somashekar ($N = 17$ and $g = 0.04$). The calculated profile using these parameters is compared to the experimental one in Fig. 10. Arbitrary values in a wide range are used as initial parameters for the refinement. All converge to the same result. These tests can be summarized as follows: $(5, 0.10) \rightarrow (17, 0.0412)$; $(10, 0.06) \rightarrow (17, 0.0413)$; $(50, 0.02) \rightarrow (17, 0.0413)$; $(100, 0.01) \rightarrow (17, 0.0419)$; $(150, 0.12) \rightarrow (17, 0.0416)$. The first number in parentheses is the value of N, the second is g.

Diffraction peaks are always superimposed on a background in an observed diffraction pattern. Accurate estimate of the background, required by the Fourier

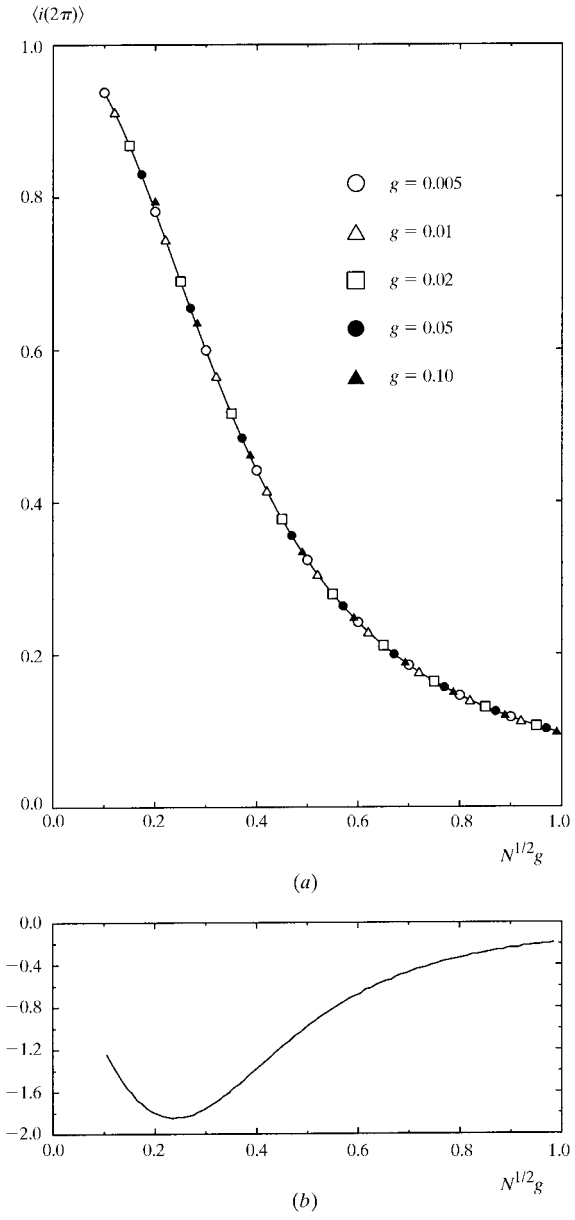

Fig. 7. (*a*) Curve of $\langle i(2\pi)\rangle$ *vs* $N^{1/2}g$. The paracrystal diffraction is a function of a single variable, *i.e.* $N^{1/2}g$. It decreases quickly with increasing $N^{1/2}g$. (*b*) Derivative of $\langle i(2\pi)\rangle$ with respect to $N^{1/2}g$. The minimum of the curve corresponds to the point of inflection of the curve in (*a*).

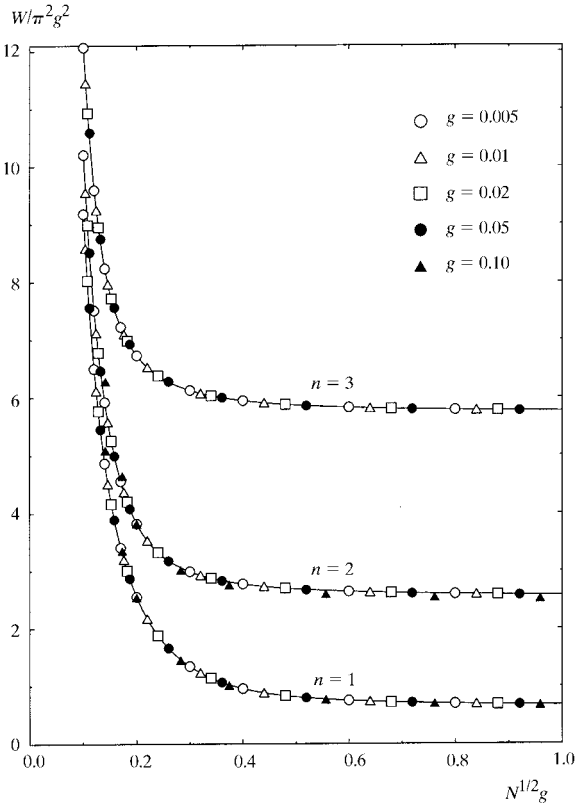

Fig. 8. Curves of W/π^2g^2 *vs* $N^{1/2}g$ for $n = 1, 2$ and 3. W is the full width at half-maximum of the diffraction profile. W/π^2g^2 is another function of the single parameter $N^{1/2}g$ for any diffraction peak.

transform technique, is a difficult task. With the refinement method we suggest here, background may be adjusted at the same time as when N and g are refined. The best values for both the background and the structural parameters (N and g) can be obtained simultaneously.

5. Discussion

The validity and the limitations of the main result of this paper, equation (15), depend on the assumptions we made in the theory. An implicit assumption is made when (14) and (15) are derived from (12) and (13), *i.e.* the degree of disorder should not be zero. In other words, β cannot be equal to 1. Otherwise, all these equations are meaningless when $\alpha = 2\pi n$ (n is an integer). Equation (15) is then not applicable to an ideal one-dimensional crystal with finite size.

The explicit assumption is that the positions of subunits in a one-dimensional paracrystal may be described by (3). These positions, however, cannot be related to an ideal infinite crystal lattice. The 'averaged lattice' extends over only a limited region, depending on the magnitude of the degree of disorder. The region is larger for a smaller g and *vice versa*.

The actual distance between any point and its Nth neighbor is $Na \pm N^{1/2}ga$. When N reaches a special value, *i.e.* $N^* = 1/g^2$, the distance becomes $N^*a \pm a$. In other words, the N^*th neighbor is no longer distinguishable from its $(N^* + 1)$th neighbor, nor its $(N^* - 1)$th one. The relation expressed by (3) completely breaks at this point. We conclude that the theory developed in this paper is valid only when $g > 0$ and $N \leq 1/g^2$.

It is interesting to compare the diffraction by a one-dimensional paracrystal with that by a helix possessing angular disorder. Both these structures are one-dimensional with cumulative disorder. The equations for both kinds of diffraction are very much alike. For example, equation (3.2) of Barakat (1987) and equation (16) of this paper are not distinguishable in form. However, their meanings are quite different. The former describes the contribution of the nth Bessel function to the layer-line intensity of the disordered helix, while the latter gives the diffraction by a one-dimensional paracrystal at the nth reciprocal-lattice point. Equation (21) of Mu *et al.* (1997) and equation (15) of this paper are also similar in form and different in meaning. One of them describes the distribution of the nth Bessel function in the reciprocal space near the layer line, while the other gives the distribution of paracrystal diffraction in the reciprocal space near the reciprocal-lattice point.

The more important difference in the diffractions by the two disordered structures is the symmetry of the diffraction. The distribution of contributions from the

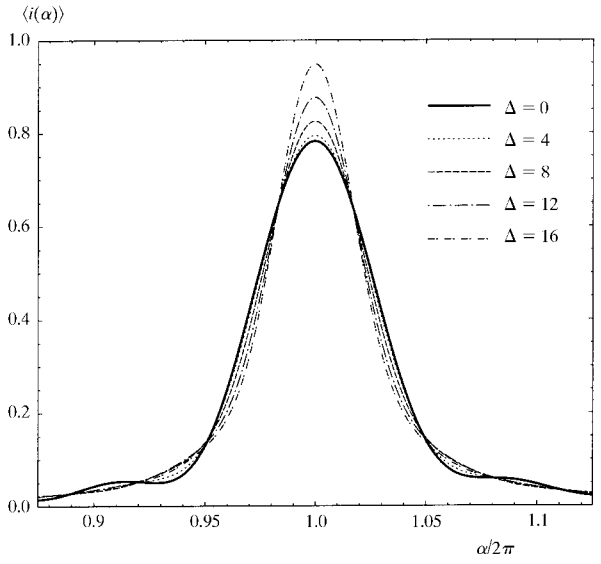

Fig. 9. The influence of size distribution on the first-order paracrystal diffraction. The average size, the degree of disorder and the shape of the size distribution ('box') are all the same for the five curves. The only difference is the breadth of the distribution, $\Delta = 0, 4, 8, 12$ and 16. The diffraction by the monodisperse paracrystal has the maximum width and the width decreases with increasing breadth of the size distribution.

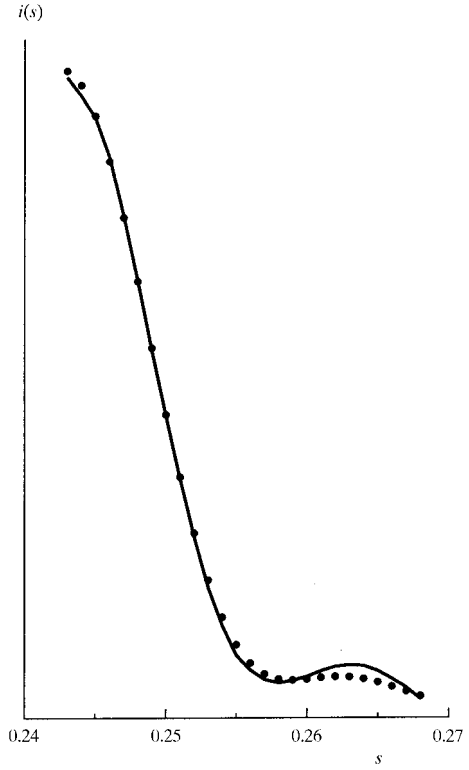

Fig. 10. Comparison of calculated and observed diffraction profiles. The solid line is a 110 reflection by polyethylene fibers, taken from Hall & Somashekar (1991). The dots represent the calculated diffraction using the size and the degree of disorder measured by the single-peak technique.

nth-order Bessel function is symmetric about the layer line. The paracrystal diffraction is, however, asymmetric about the reciprocal-lattice point and the diffraction position even deviates from the latter. Equation (3.2) of Barakat always gives the maximum of the intensity, while equation (16) of this paper may not give the maximum owing to the peak shift.

This discrepancy is because of the different definitions of α and β in the two cases. As shown in equations (9) and (10) of this paper, the parameters α and β are dependent. They are independent for the disordered helix, as shown in equations (13) and (14) in Mu *et al.* (1997). Actually, the symmetry of the diffraction depends on those of the trigonometric and exponential functions in the equations. For a one-dimensional paracrystal, $\cos\alpha$ and $\cos N\alpha$ are symmetric while β and β^N monotonously decrease with α^2. As a result, the diffractions by a one-dimensional paracrystal are asymmetric about their maxima and the asymmetry causes the aperiodicity of positions of maxima at last. For the disordered helix, the exponential functions are α independent, *i.e.* they are symmetric also. Their diffractions are, then, symmetric about their maxima and no peak shift is observed.

The method to measure the paracrystal size and the degree of disorder, suggested in this paper, is applicable to monodisperse system. It may be applied also to a polydisperse system to obtain an 'averaged' size and the degree of disorder. This kind of 'averaged' size, however, is usually larger than $\mathcal{N}$, given by equation (32). Information about crystallite-size distribution is very important for a polydisperse system. A new method to measure the distribution has been proposed recently (Bodor *et al.*, 1996). A refinement method for the measurement may be developed when formulas for the diffraction profile for other size distributions are available in addition to (34) and (35) for the 'box' distribution.

I would like to thank Dr Lee Makowski for helpful discussions and for comments concerning the manuscript. This work was supported by the National Institutes of Health, grant HL 28381, and a grant from the National Science Foundation.

References

Baltá-Calleja, F. J. & Hosemann, R. (1980). *J. Appl. Cryst.* **13**, 521–523.
Baltá-Calleja, F. J. & Vonk, C. G. (1989). *X-ray Scattering of Synthetic Polymers*, pp. 129–174. New York: Elsevier.
Barakat, R. (1987). *Acta Cryst.* A**43**, 45–49.
Bodor, G., Gall, S., Häberle, K. D., Lode, U. & Wilke, W. (1996). *J. Polym. Sci. Polym. Phys.* **34**, 485–496.
Bonart, R., Hosemann, R. & McCullough, R. L. (1963). *Polymer*, **4**, 199–211.
Brämer, V. R. (1975). *Acta Cryst.* A**31**, 551–560.
Gradshteyn, I. S. & Ryzhik, I. M. (1980). *Tables of Integrals, Series and Products*, p. 31. New York: Academic Press.
Guinier, A. (1939). *Ann. Phys. (Leipzig)*, **12**, 161–237.
Hall, I. H. & Somashekar, R. (1991). *J. Appl. Cryst.* **24**, 1051–1059.
Hosemann, R. (1962). *Polymer*, **3**, 349–392.
Hosemann, R. & Bagchi, S. N. (1962). *Direct Analysis of Diffraction by Matter.* Amsterdam: North-Holland.
Mu, X.-Q., Makowski, L. & Magdoff-Fairchild, B. (1997). *Acta Cryst.* A**53**, 55–62.
Press, W., Flannery, B. P., Teukolsky, S. & Vetterling, W. T. (1986). *Numerical Recipes.* Cambridge University Press.
Scherrer, P. (1918). *Göttinger Nachrichten*, **2**, 98–103.
Somashekar, R., Hall, I. H. & Carr, P. D. (1989). *J. Appl. Cryst.* **22**, 363–371.
Vainstein, B. K. (1966). *Diffraction of X-rays by Chain Molecules.* Amsterdam/London/New York: Elsevier.
Warren, B. E. (1959). *Prog. Met. Phys.* **8**, 147–202.
Warren, B. E. & Averbach, B. L. (1950). *J. Appl. Phys.* **21**, 595–599.
Zernike, F. & Prins, J. A. (1927). *Z. Phys.* **41**, 184.